SINDA/FLUINT and Thermal Desktop Multi-Node Settled and Unsettled Propellant Tank Modeling of Zero Boil Off Test

Barbara Sakowski, Daniel M. Hauser
NASA/Glenn Research Center

M. Kassemi
National Center for Space Exploration Research (NCSER)

Cleveland, OH, 44135, USA

I. Introduction

Cryogenic propellant storage tank self-pressurization involves complex physical phenomena which are usually analytically modelled via complex multidimensional CFD codes. Unfortunately these codes, even when modelling axisymmetric domains, may takes weeks or longer to obtain transient pressure and temperature information for relatively short periods of time (several seconds to several hours). Propellant tank storage end-to-end mission simulations can last a duration of days to weeks to months. Multi-node modelling of propellant tanks is a viable alternative to traditional CFD modelling and presents the advantage of greatly reduced run times on the order of hours and days compared to the weeks or longer for CFD codes. A multi-node model represents the fluid within the storage tank, as well as the storage tank itself, as a fluid-thermal network. This type of setup is not necessarily geometrically based. This can be accomplished using a commercial generalized fluid-thermal network code, such as SINDA/FLUINT (SF). The advantage of using a fluid-thermal network code like SF lies in its extensive ability to model the external environment of the storage tank through the graphical user interface, Thermal Desktop (TD). The total heat load into the tank may be a function of heaters and a complex radiative environment as well. Thermal Desktop may be used to address the detailed radiative environment of the tank as well as building a geometrically accurate depiction of the storage tank itself.

A general purpose SF stratified tank model was created to simulate self-pressurization of cryogenic storage tanks[1]. The model can be set up as a multi-nodal representation (one, two, or three dimensional). The state of the fluid in the tank can be settled under conditions of normal gravity or unsettled in a microgravity environment. Furthermore, the tank wall and its exterior environment can also be modelled in TD with full geometric detail. Also an interface with TD was created so that detailed geometric tank wall modelling and complex radiative thermal environments could be included.

This model was validated with Zero-Boil-Off Test (ZBOT) data[2]. The ZBOT models include self-pressurization under 1g and microgravity with a strip heater and a surrounding vacuum jacket. The modelling effort employs a simple SF multi-nodal representation of the tank wall and its exterior environment as well as a detailed TD geometric representation of the tank wall and its external radiative environment.

II. Model Details

Model Background

A general purpose SF stratified tank model was created to simulate self-pressurization of storage tanks. The model can be set up as one, two, and three dimensional, as well as the tank being in settled conditions under normal gravity and unsettled conditions in a zero or micro-gravity environment. The SF model employs the use of stratified layers, i.e. SF LUMPS, in the vapor and liquid regions. The model can be used for analyzing general purpose stratified tanks that may incorporate the following features:

- Multiple or singular LUMPS in the liquid and vapor regions of the tank
- Real gases (also mixtures) and compressible liquids

- Venting, pressurizing, and draining
- Condensation and evaporation/boiling
- Wall heat transfer (Boiling, Convection, Radiation)
- Elliptical, cylindrical, and spherical tank geometries
- Internal tank wall to wall radiation, and external tank wall radiation to the environment

Extensive user logic and use of the SF/TD REGISTER DATA BLOCK, allows for tailoring of the above features to specific cases.

Zero-Boil-Off-Test Set Up

The ZBOT tests were conducted in microgravity and a 1g environment. The microgravity environment was held to approximately 5E-6 m/s^2. A strip heater, applied to the outer tank wall, was comprised of acrylic and stainless steel as shown in Figure 1. The heater supplied 0.5 W in microgravity and 1.0 W in the 1g environment. In the jet mixing cases, fluid was drawn from the bottom of the tank and reentered through the inlet nozzle at the bottom of the tank. A vacuum jacket was used to isolate the tank from the environment, Figure 2. The vacuum jacket was comprised of aluminum and the windows are glass. A vacuum was formed inside the vacuum jacket to prevent heat transfer by conduction or convection. The area-averaged temperature of the vacuum jacket was controlled in order to control the radiative environment and thus the heat transfer into the tank.

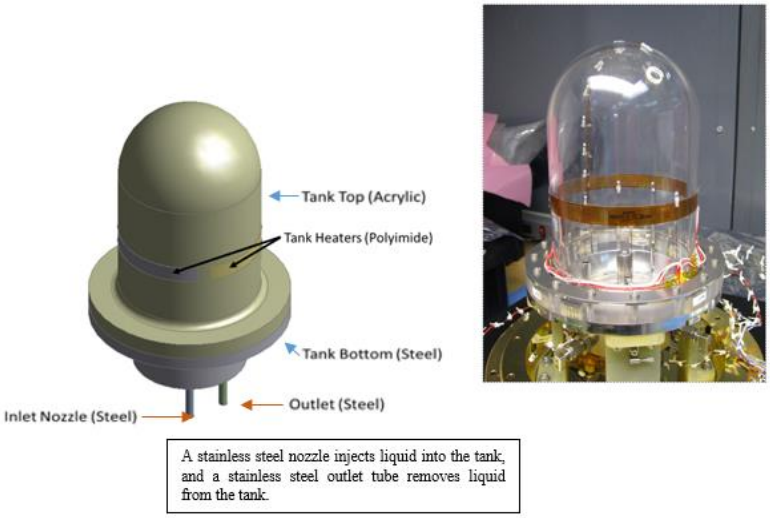

Figure 1: ZBOT Tank

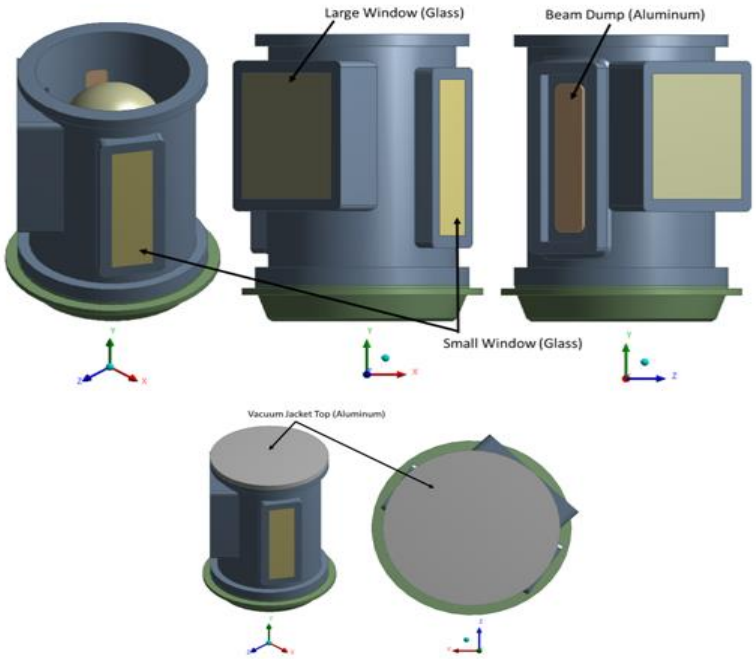

Figure 2: ZBOT Vacuum Jacket Assembly

Thermal Desktop and SINDA/FLUINT Modelling

A general purpose thermally stratified tank model was creating using SINDA/FLUINT[1]. The model can be set up as a multi-nodal representation in one, two, or three dimensions in gravity as well as microgravity. The model can also incorporate jet mixing. In all cases presented the stratified fluid was represented as one dimensional. A basic schematic of a one dimensional stratified tank is shown in Figure 3. Figure 4 illustrates a multi-nodal representation when jet mixing is modelled.

An interface to Thermal Desktop and the SINDA/FLUINT stratified tank model was created so that a complex geometry, which may include a detailed radiative environment, can be used instead of a non-geometric, lumped thermal node representation of the tank wall. The TD model of the tank wall is represented in Figure 5, where there are 12 nodes that represent the acrylic portion of the tank and the stainless steel tank bottom, or skirt, has a detailed nodalization. This was done to illustrate that the interface can handle both simple and complex discretizations. In the SF multi-nodal lumped geometry wall representation, 40 nodes were used in the vapor wall section, and 50 nodes were used in the liquid wall section.

For all the test cases modelled, the SF stratified tank model used 40 LUMPS to represent the vapor ullage and 75 LUMPS to represent the liquid. Previous experience modelling tank stratification has shown that this model required at least 20 vapor LUMPS and 30 liquid LUMPS to obtain reasonable results quickly. Discretizing the liquid past 100 LUMPS gained no more significant changes in the results (relative to 75 liquid LUMPS), but did start impeding model run times.

It should be noted that in microgravity, since a one dimensional multi-nodal representation of the fluid is being utilized, the vapor ullage is modelled as though it were an ullage and not a spherical bubble moving about the tank. The interface area used for heat transfer between the liquid and vapor is based on the diameter at the interface between the

liquid and the vapor. Currently there is no methodology in the code to track the vapor liquid interface as the vapor bubble moves about the tank.

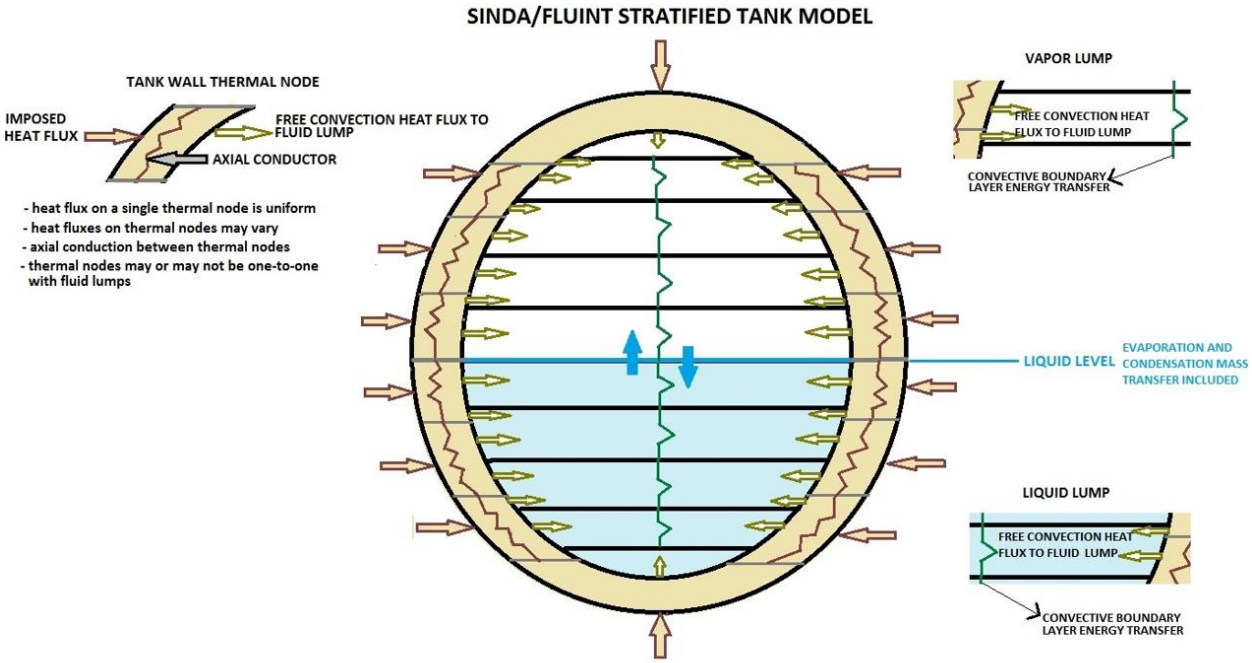

Figure 3: SINDA/FLUINT Stratified Tank Showing Liquid/Vapor Interface, Tank Wall with Thermal Conductors, Free Convective Heat Transfer and Associated Boundary Layer Energy Transfer

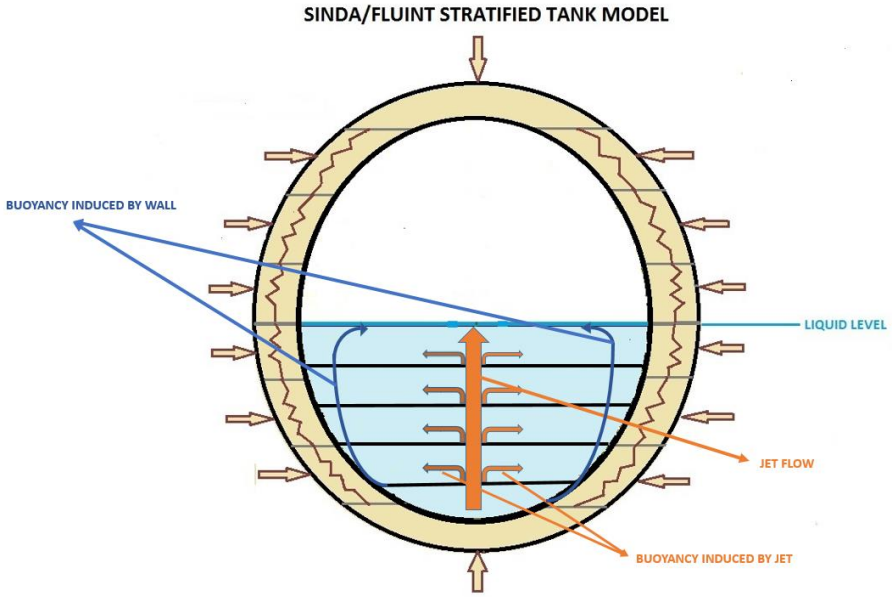

Figure 4: SINDA/FLUINT Stratified Tank Showing Liquid/Vapor Interface, Tank Wall with Thermal Conductors, Jet Flow, and Buoyancy Induced by Jet and Wall

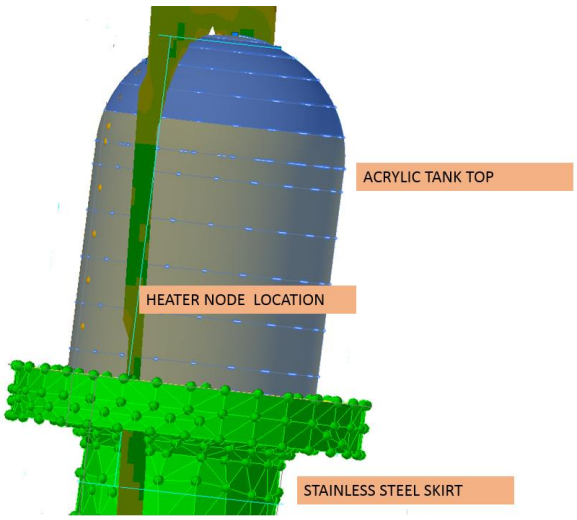

Figure 5: Thermal Desktop Geometric Representation of Tank

Radiation and Perfuoropentane

The fluid inside the tank, perfluoropentane, is not opaque throughout the entire IR spectrum. A plot of perfluoropentane transmittance versus wave number is shown in Figure 6. A rough integration of the transmittance through visual inspection of Figure 6 is illustrated in Figure 7. The regions integrated are the near and middle IR regions. Total transmittance through these wavelength regions is approximately 25%. Figure 8 illustrates probable transmittance in the far IR region. A rough integration of the transmittance through this wavelength region, assuming a 90% transmittance, yields a total transmittance of approximately 13%. Thus the total transmittance through the entire IR range is approximately 38%, Figure 9. Finally no information could be found to determine if the transmittance through the vapor differed from the transmittance through the liquid.

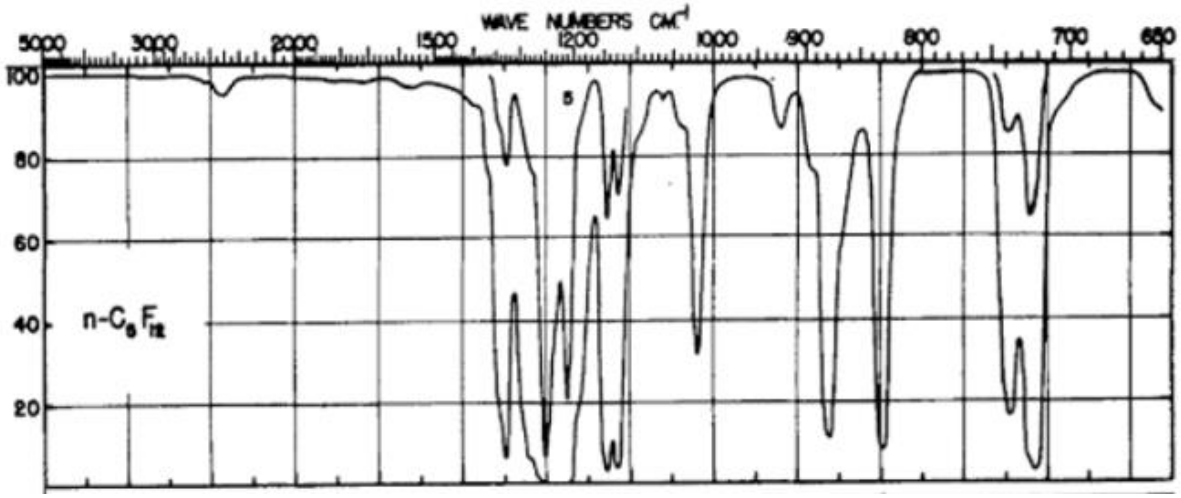

Figure 6: Perfluoropentane Transmittance Versus Wave Number[4]

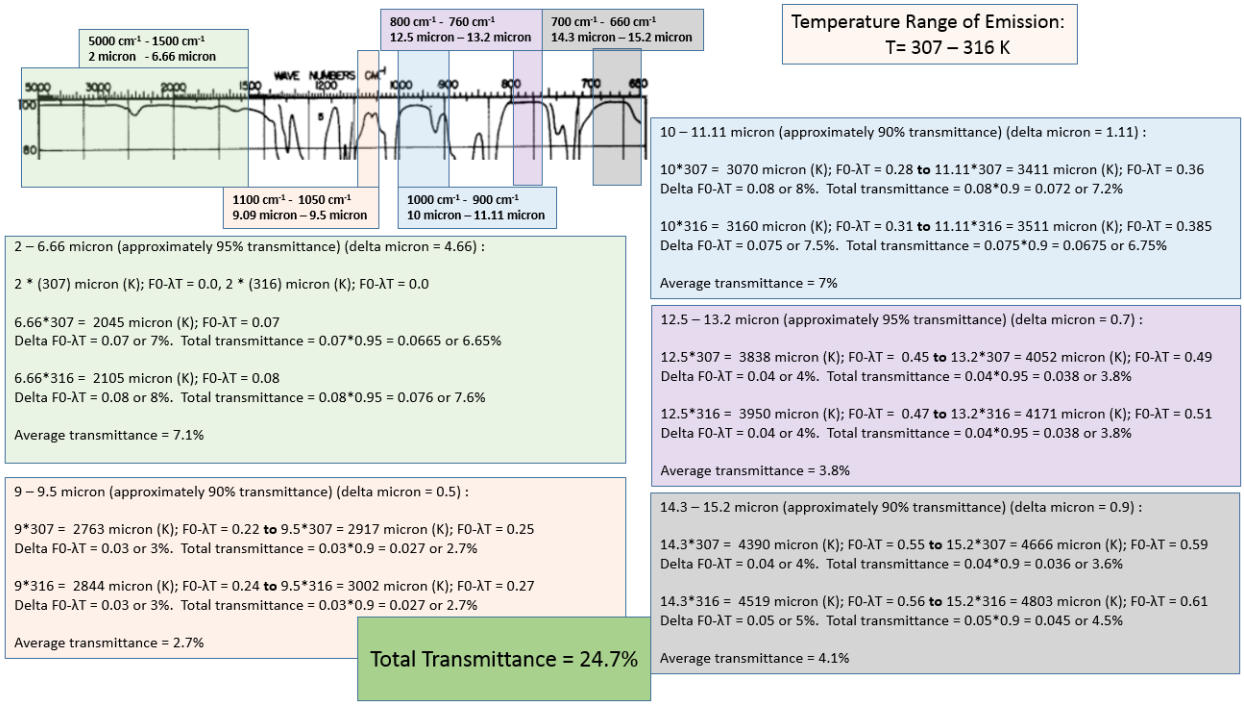

Figure 7: Transmittance Integration of Perfluoropentane in the Near and Middle IR Regions

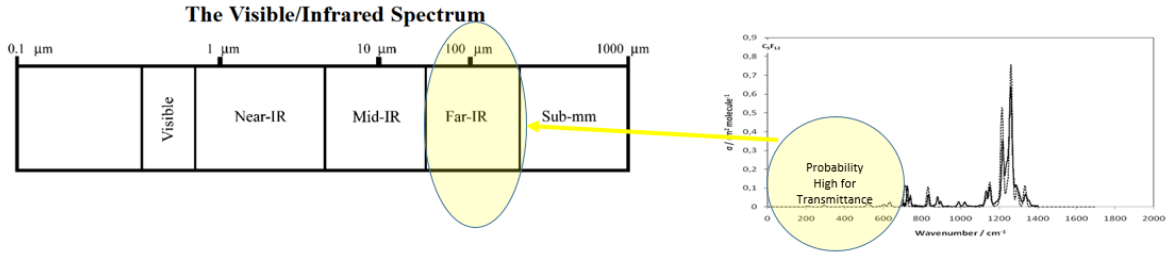

Sigma is the absorption cross section in cm^2 $molecule^{-1}$averaged over a 10 cm^{-1} interval around the wavenumber. Absorption cross section is a measure for the probability of absorption to occur.

Figure 8: Probable Transmittance of Perfluoropentane[5] in the Far IR Region

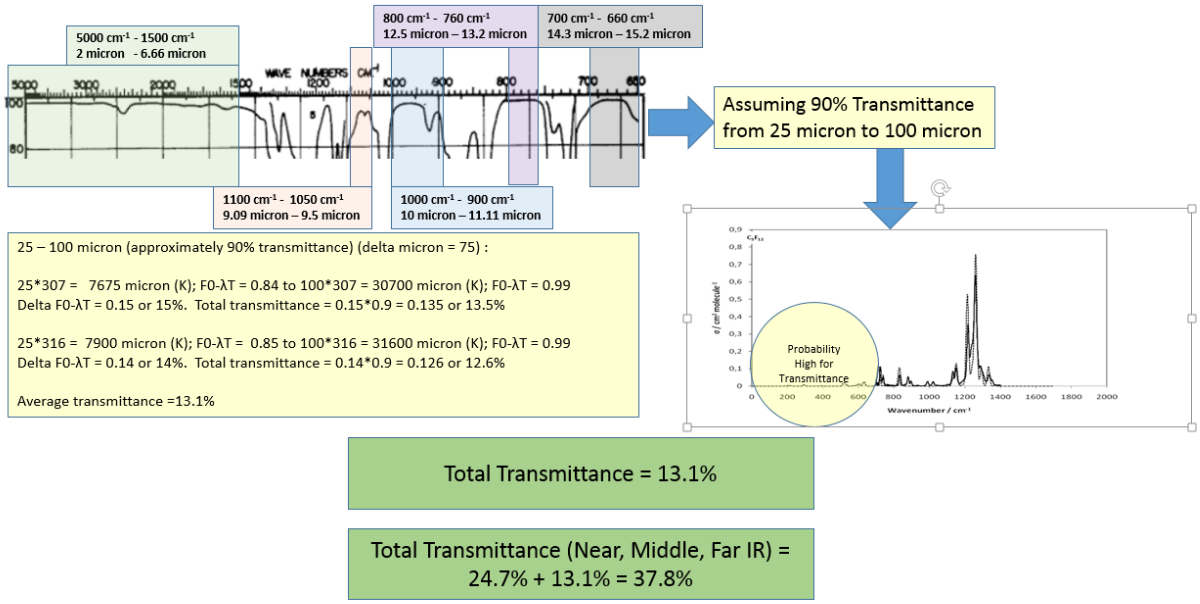

Figure 9: Transmittance Integration of Perfluoropentane in the Far IR Region

Wall Radiation

Given that perfluoropentane is not completely opaque, internal tank wall to wall radiation was included. The radiation exchange from the outer tank wall to the vacuum jacket was also included. The model which included the TD interface had a complete geometric representation of the tank and vacuum jacket. TD generated all the radiation conductors internal and external to the tank wall. In the SF model, subroutines were written to model internal wall to wall radiation as well as external tank radiation to the vacuum jacket. Since a simplistic representation of the vacuum jacket was being implemented in the SF model, an area-averaged emissivity of the vacuum jacket consisting of window glass and aluminum was used. Table 1 shows the emissivities used.

Material	Emissivity
Stainless Steel	0.44
Aluminum (Polished Gold)	0.02
Acrylic	0.94
Window Glass	0.95
Heater (Polyimide)	0.75

Table 1: Emissivities of Surfaces

Wall Buoyancy

Convection Time in Microgravity

The microgravity test pressure data showed a significant delay in pressure rise at the start of the test. It was surmised that in microgravity the free-convection/buoyancy has an effect on self-pressurization but there is a delay time for the convection to balance the conduction into the thermal boundary layer. The "time to convect" expression, past which convection is applicable was derived, Equation 1. A scale analysis by Bejan[3] is further modified to include appropriate

length scales and exponentiation analogous to the boundary layer empiricisms for heat transfer, thickness, and velocity.

$$Tcv = (C \nu H/(g \beta \Delta T_w \alpha))^{(2/5)} \quad (1)$$

$$C \approx (D/H)^{(3/5)} \quad (2)$$

Length Scales

When modelling free convective effects in a stratified tank it is important to scale the boundary layer empiricisms with the appropriate length scales such as tank diameter and tank height. For example an appropriate length scale for the liquid region of the tank would include the interface diameter and the liquid level. These values would be used in Equation 2 above for D and H respectively. The vapor ullage would also use the interface diameter also but use the height of the vapor ullage (relative to the liquid level) for the value of H.

The ZBOT cases involve a special case where there is a strip heater, providing a localized heat rate on a small portion of the tank wall. This creates another length scale, the width of the strip heater, to use as the value of H in Equation 2. Yet another length scale is used to help determine the value of C in Equation 2. The time that each fluid LUMP has passed the critical time, tcv, may differ so the sum total incremental height of all the LUMPS that are free convecting is calculated as a function of time. Ultimately the sum total height reaches the total height of the region (i.e., the liquid level height for the liquid region). This length scale is used as an interpolation factor, F, on Equation 2 so that there is a smooth transition from the conduction heat transfer regime to the free convective heat transfer regime:

$$C \approx F (D/H_{str})^{(3/5)} \quad (3)$$

$$F \approx (\text{Total Lump Convecting Height}/H)^{(3/5)} \quad (4)$$

Jet Buoyancy

In the jet mixing case with normal gravity, it was important to model the buoyancy effects created by the cooler jet flow. While the wall buoyancy creates an upward heated flow along the wall, the jet creates a downward cooled flow along the center part of the tank. This buoyancy force could impede the flow of the jet to the interface. The buoyancy boundary layer and corresponding flow rate it produces is calculated analogously to the buoyancy boundary layer and flow rate induced by the tank wall. The following correlation for Nusselt number is used[3]:

$$Nu \sim 0.6\ Ra^{(0.2)} \qquad 10^5 < Ra < 10^{13} \quad (5)$$

The Raleigh number in these correlations is based on the respective height of each LUMP. Imbedded in the Rayleigh number is Equation 3. It should be noted that the boundary layer itself is not modeled. There is no LUMP that wholly represents the boundary alone, that is, has the volume and thickness associated with the boundary layer at any given point along the tank wall. The LUMP nearest the tank wall is assumed to contain the boundary layer, and all the characteristics of the boundary layer at the location of that LUMP are calculated based on its thermodynamic state. In a one dimensional multi-nodal model there is only one LUMP near the wall (i.e., there are no radial LUMPS). The boundary layer characteristics calculated for each LUMP are:

- Characteristic velocity
- Boundary layer thickness
- Buoyancy driven volume flow rate

The characteristic velocity as well as the boundary layer thickness is obtained by a general scaling analysis[3].

$$U \sim \alpha / H\ Ra^{(2/5)} \quad (6)$$

$$\delta \sim Pr^{(0.5)} (H\ Ra^{(-1/5)}) \quad (7)$$

The effects of the boundary layer are modeled as an energy exchange between the LUMPS using SINDA/FLUINT FTIES. This energy is equivalent to the convective heat of the boundary layer. These energy ties flow "upward" along the tank wall.

In the case of the buoyancy flow caused by the jet, the wall temperature is replaced by the temperature of the jet. The SINDA/FLUINT energy FTIES still flow "upward" at a rate:

$$Q_j = (m_j - m_b)(h_{LU} - h_j) \quad (8)$$

Once the jet buoyancy boundary layer is developed it creates a downward flow which impedes the flow of the jet moving upward toward the vapor/liquid interface. The flow rate that impedes the jet flow rate, m_b, is subtracted from the flow rate that ultimately hits the interface. The energy corresponding to the subtracted differential flow rate for each LUMP is applied to that LUMP, as illustrated in Figure 4. The arrows corresponding to the buoyancy induced by the jet show energy leaving the main jet flow and entering the corresponding LUMP.

Jet Impingement Heat Transfer at Vapor/Liquid Interface

The heat transfer that occurs at the vapor/liquid interface due to the jet impingement is taken from Lin et al.[6] The Nusselt number is defined by:

$$Nu = (\rho c_p U_j Xa\ St)\ D / k \quad (9)$$

$$St = 0.0198\ Pr^{(-0.33)}\ (1.0 - 0.5Ja) \quad (10)$$

$$Xa = 1.0 + (D_{int}/D_j)^{2.0}\ 0.0198\ Pr^{(-0.33)}\ (V_{int}/U_j) \quad (11)$$

$$V_{int} = U_j\ D_j/D_{int}\ (10.04\ (0.24) - Xb\ djet/\ D_{int}) \quad (12)$$

$$Xb = 7.14(0.24) - 3.06(0.34) \quad (13)$$

III.Results

ZBOT Jet Mixing Case 905 1g

ZBOT Case 905 was conducted in a 1g environment. The fill level was 90% and there was no heat added to the system. The jet flow rate was 2.57 g/s. Pressure results are shown in Figure 10. Agreement with test data is quite good when the buoyancy of the jet is included. When buoyancy is not included the pressure in the tank immediately decreases since there is no induced buoyancy flow from the jet to impede the jet reaching the interface. This is further illustrated in Figure 11 and Figure 12 which shows the temperature distributions in the stratified liquid. Figure 11 shows the temperature profiles with the buoyancy flow enabled. The temperature of LUMP 115 which is at the bottom of the tank is immediately cooled, since the buoyancy flow forces some of the jet flow downward toward the bottom of the tank. Eventually the top liquid LUMP near the vapor/liquid interface catches up in cooling incrementally through the stratified layers. If no buoyancy effect from the jet is modelled, the top liquid LUMP 41 immediately cools from the impinging jet at the vapor/liquid interface (Figure 12).

Also illustrated in Figure 10, is the initial drop in pressure due to the unencumbered jet hitting the interfacing. The pressure than increases due to the buoyancy interfering with the jet hitting the interface.

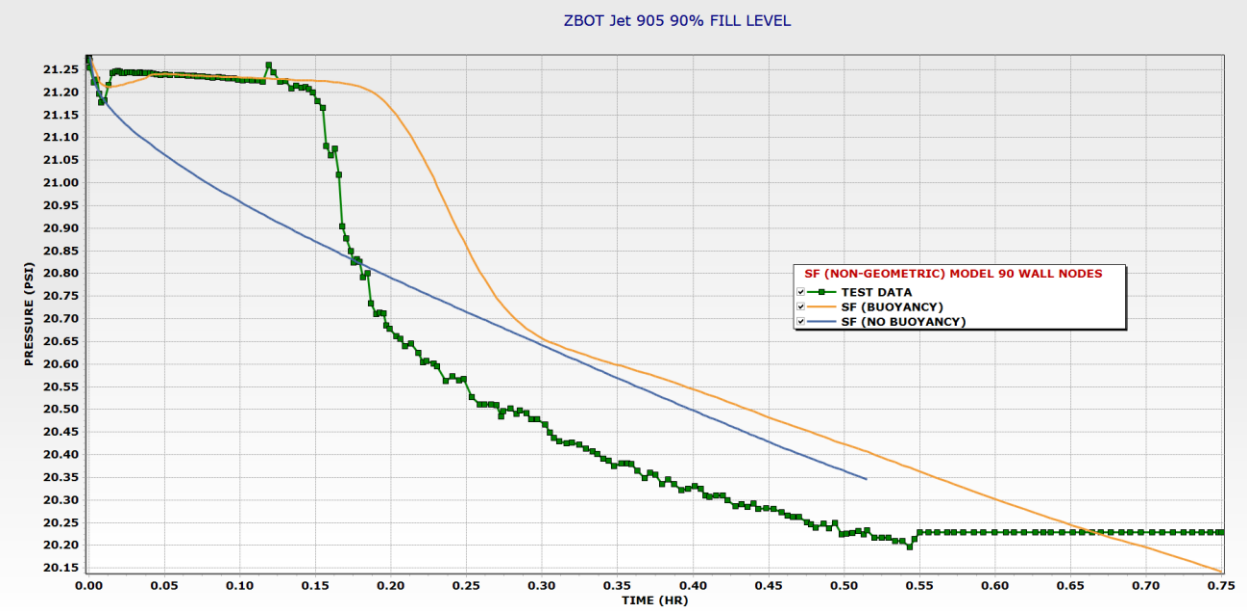

Figure 10: ZBOT Jet Mixing Case 905 1g Pressure Versus Time for Test Data, SF Jet Buoyancy Model, SF Jet with No Buoyancy Model

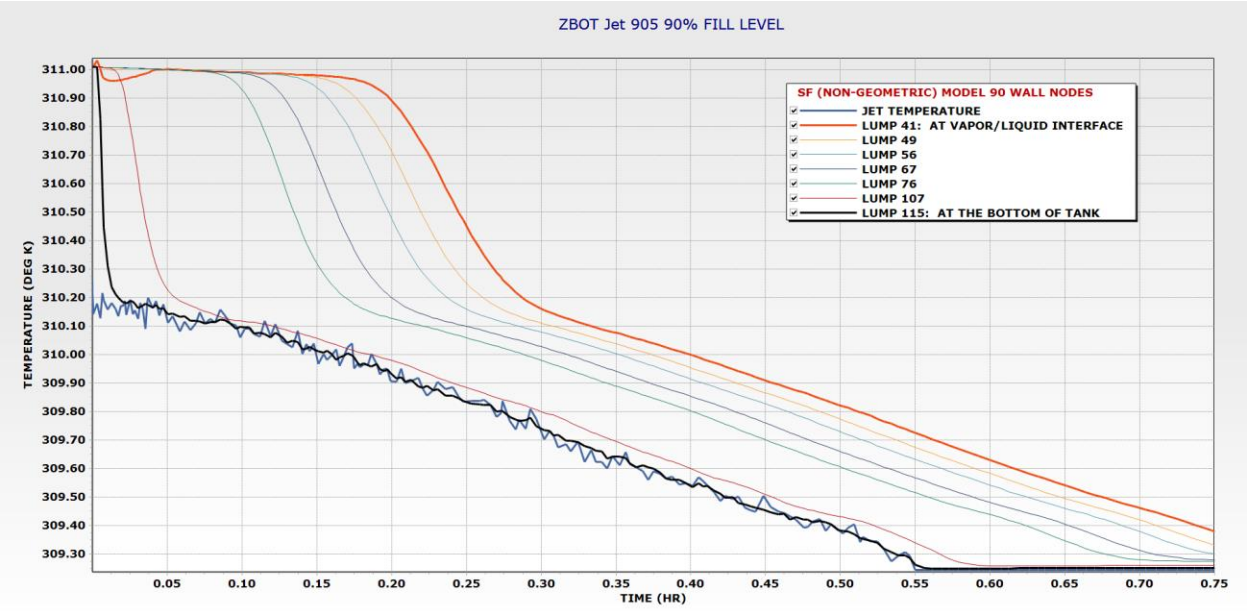

Figure A11: ZBOT Jet Mixing Case 905 1g Temperature Versus Time for SF Jet Buoyancy Model

Figure 12: ZBOT Jet Mixing Case 905 1g Pressure Versus Time for SF Jet with No Buoyancy Model

ZBOT Jet Mixing Cases 205, 206, 207 Microgravity

ZBOT microgravity jet mixing cases 205, 206, and 207 jet mass flow rates and fill levels are illustrated Table 2.There was no heat rate applied to the walls in these cases. Pressure Results for these cases are shown in Figures 13 through 15. All cases show that the SF model results compare well with test data.

ZBOT Jet Mixing Cases Microgravity	Jet Flow Rate (g/s)
205 76.4% Fill	3.85
206 76.64% Fill	3.86
207 76.82% Fill	3.84

Table 2: ZBOT Jet Mixing Cases

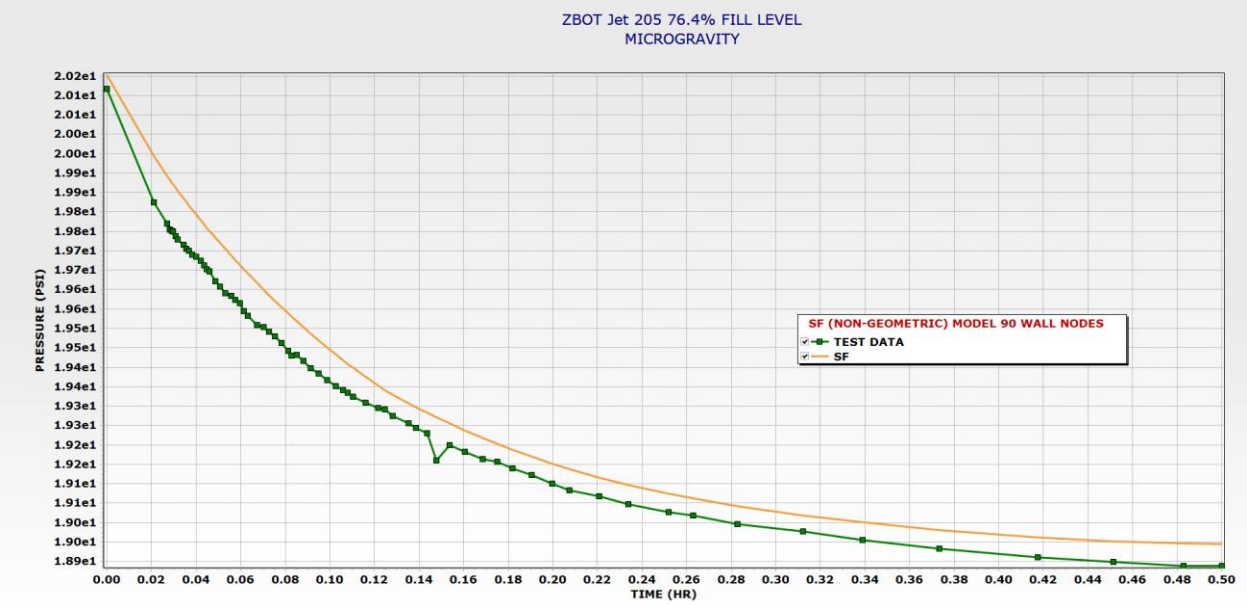

Figure 13: ZBOT Jet Mixing Case 205 Microgravity Pressure Versus Time for SF Model

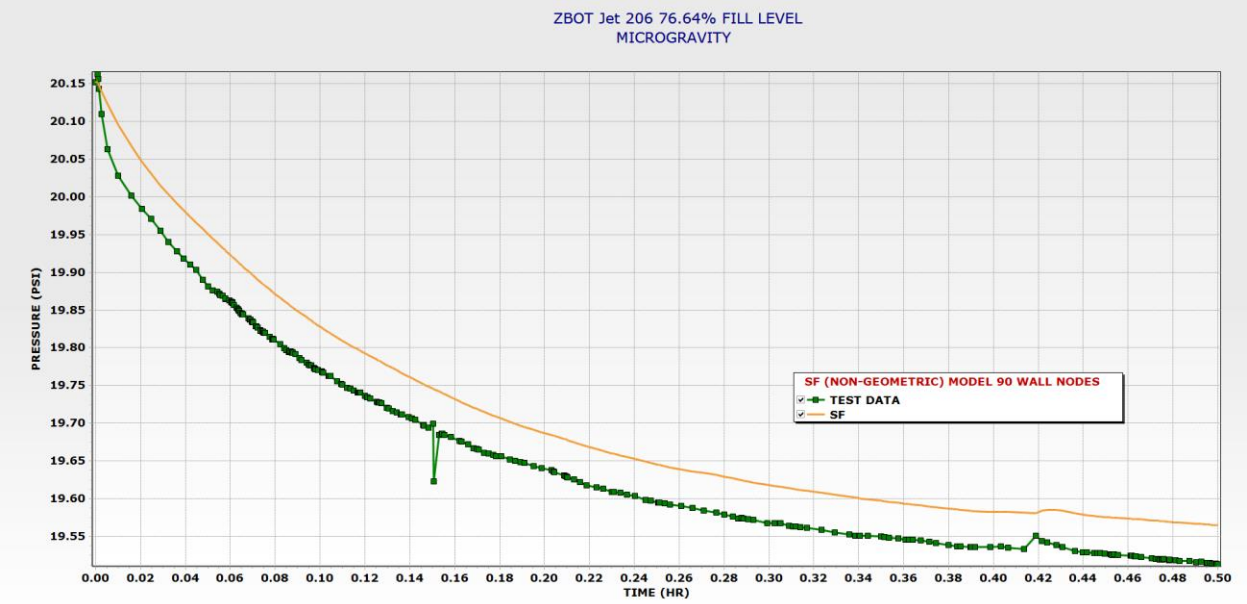

Figure 14: ZBOT Jet Mixing Case 206 Microgravity Pressure Versus Time for SF Model

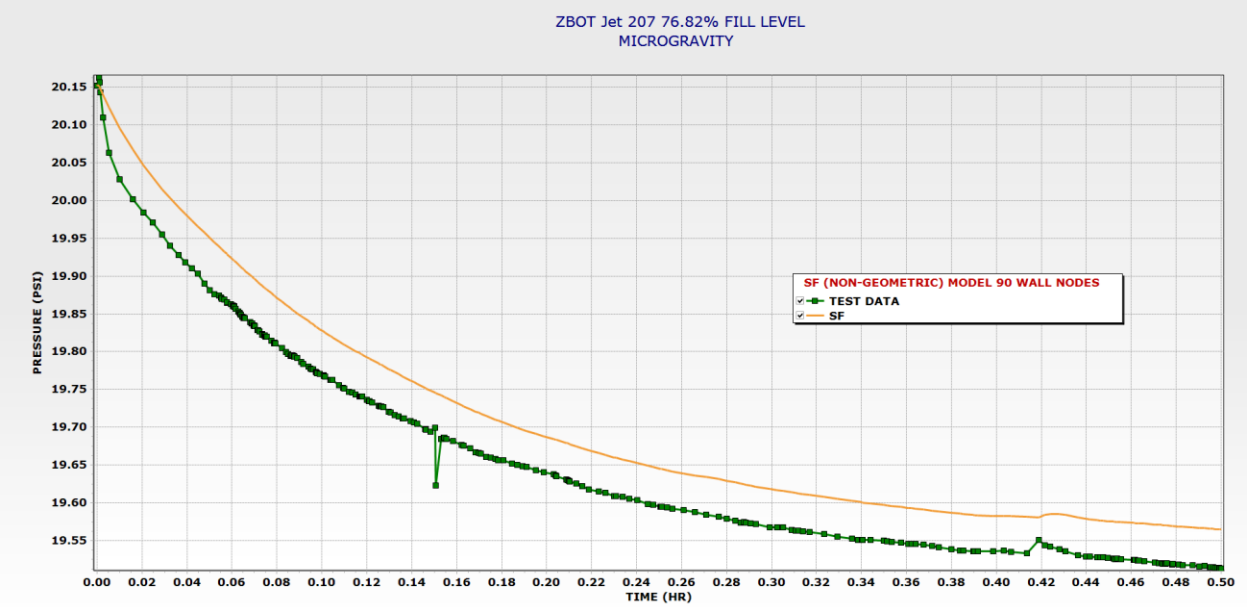

Figure 15: ZBOT Jet Mixing Case 207 Microgravity Pressure Versus Time for SF Model

ZBOT Self-Pressurization Case Microgravity 0.5 Watts Strip Heater

The fill level for this ZBOT self-pressurization case under microgravity was 80.82%. Figure 16 shows that the amount of radiation transmitted through the perfluoropentane had an effect on the model's pressure results. The probable radiation transmission through perfluoropentane, as discussed earlier, can reasonably be anywhere between 20% and 40%. The pressure results at 20% and 40% transmission from the SF model are quite agreeable to the test data. Allowing zero transmission (i.e. no internal wall to wall radiation) yielded the poorest pressure result, relatively speaking. Although this result at zero transmission is not all too bad on its own.

Figure 17 shows the pressure results from the TD model for zero radiation transmission and 100% radiation transmission through perfluoropentane within the tank. They both compare reasonably well with the test data. Figure 18 compares the pressure results from the TD model and the SF model, at the same radiation transmission rates. They also compare reasonably well to each other. Minor difference occur mostly due to the fact that the TD model only has 15 thermal nodes representing the wall in the acrylic portion of the tank. The SF model has approximately 100 thermal nodes representing the wall in the acrylic portion of the tank.

The pressure results incorporating the delay time for buoyancy to begin compared to having the convective heat transfer start immediately are shown in Figure 19. These pressure results are from the SF model using a 40% radiation transmission rate through perfluoropentane. Pressure results incorporating the delay time for convective heat transfer to begin agrees better with the test data. In microgravity this effect is prominent. Initially, conduction is the dominant rate of heat transfer in the tank until the characteristic time is reached for convection to dominate.

Figure 20 shows the wall temperature at the heater location as a function of time for the TD model compared to the test data. Results from the TD model are for zero radiation transmission and 100% radiation transmission through perfluoropentane within the tank. Temperature results for each transmission rate compare reasonably well to test data.

Figure 21 shows the wall temperature at the heater location as a function of time for the SF model compared to the test data. Results from the SF model are for zero radiation transmission and 20%, 40%, and 100% radiation transmission through perfluoropentane within the tank. Temperature results for each transmission rate compare reasonably well to test data. In the case of zero internal wall to wall radiation, the temperature at the location of the

heater does have a greater transient overshoot before normalizing later in time. This is not seen in the TD model results, perhaps because the node representing the heater location has a larger mass associated with it than in the SF model.

Finally Figure 22 compares the TD and SF models in terms of calculating the radiation heat exchange between the outer tank wall and the vacuum jacket, as well as the total amount of heat entering the tank. These values compare reasonably well. Again any initial transient differences are most likely due to the difference in tank wall nodalization.

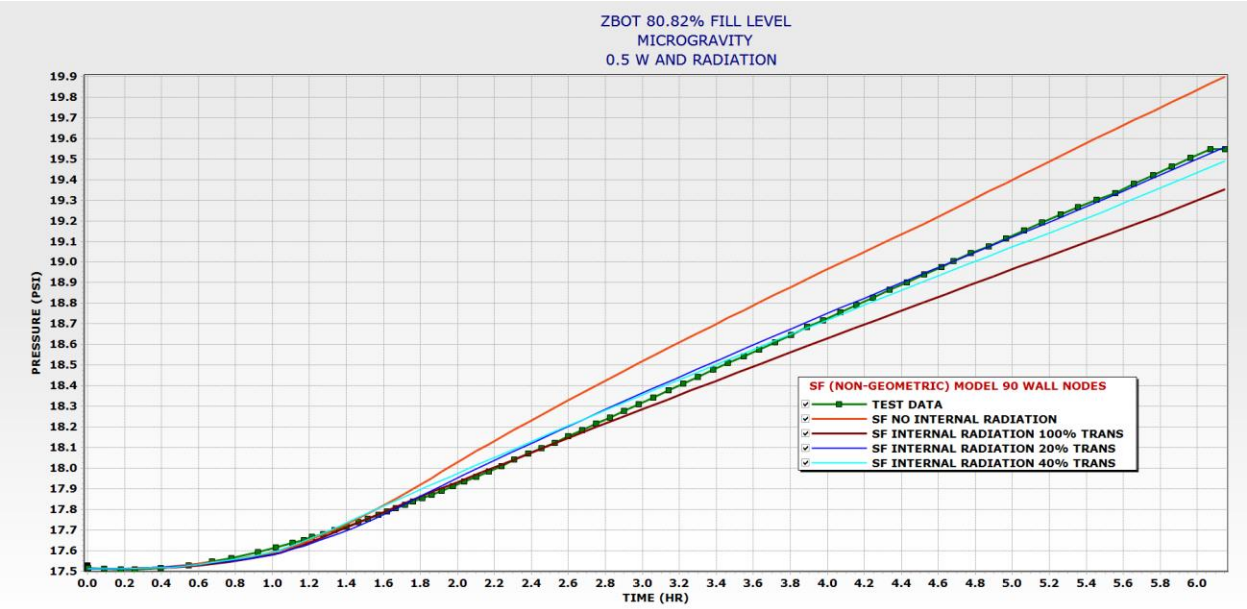

Figure 16: ZBOT Self-Pressurization Case Pressure Versus Time for Various Rates of Radiation Transmission through Perfluoropentane for SF Model

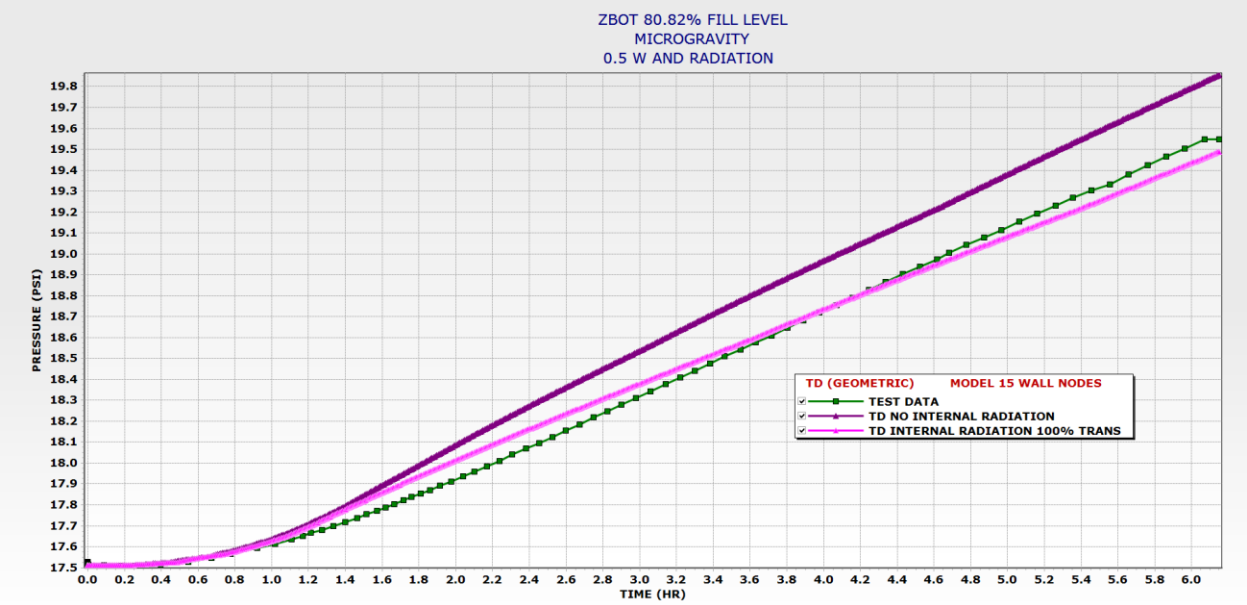

Figure 17: ZBOT Self-Pressurization Case Pressure Versus Time for Various Rates of Radiation Transmission through Perfluoropentane for TD Model

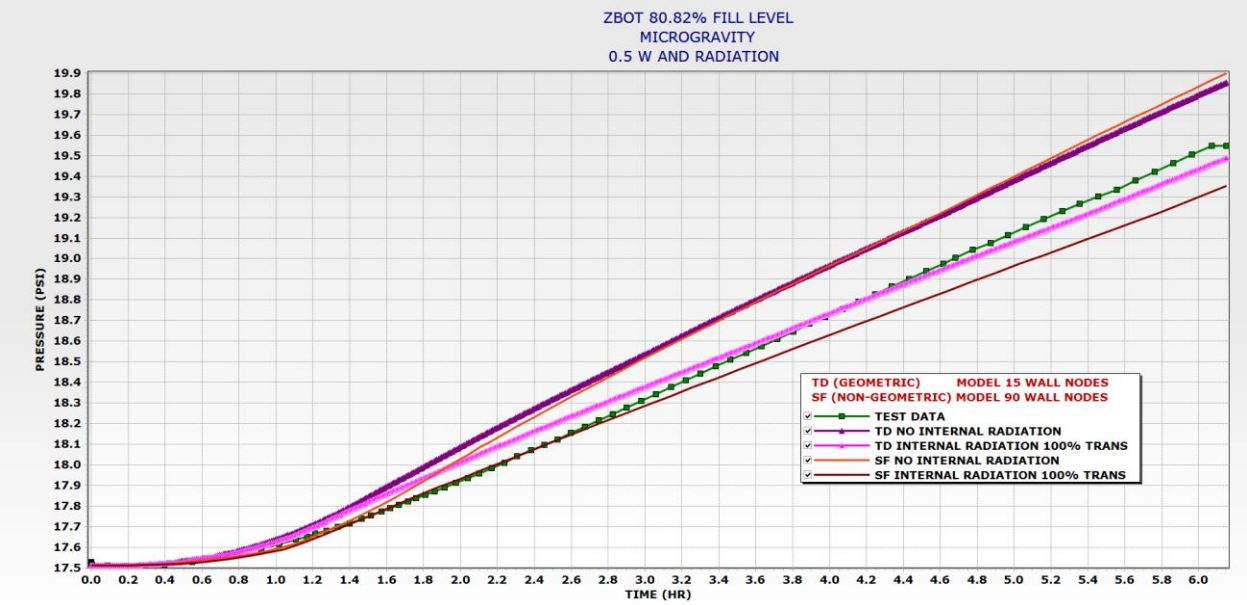

Figure 18: ZBOT Self-Pressurization Case Pressure Versus Time for 0% and 100% Rates of Radiation Transmission through Perfluoropentane for TD Model and SF Model

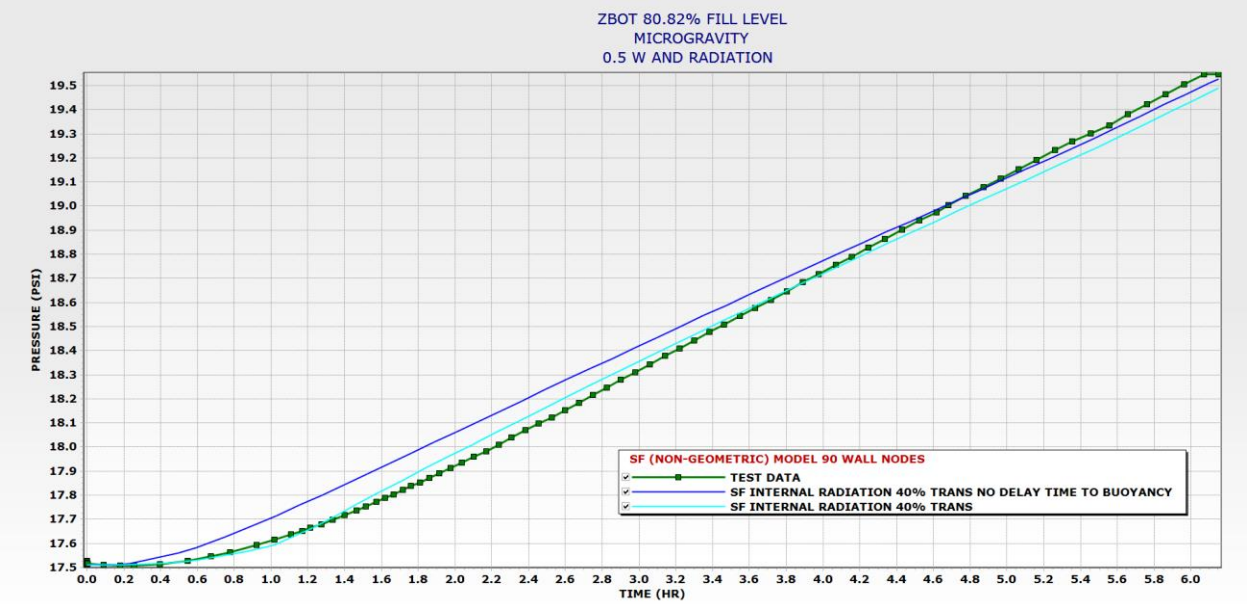

Figure 19: ZBOT Self-Pressurization Case Pressure Versus Time with and without Delay Time to Buoyancy for SF Model

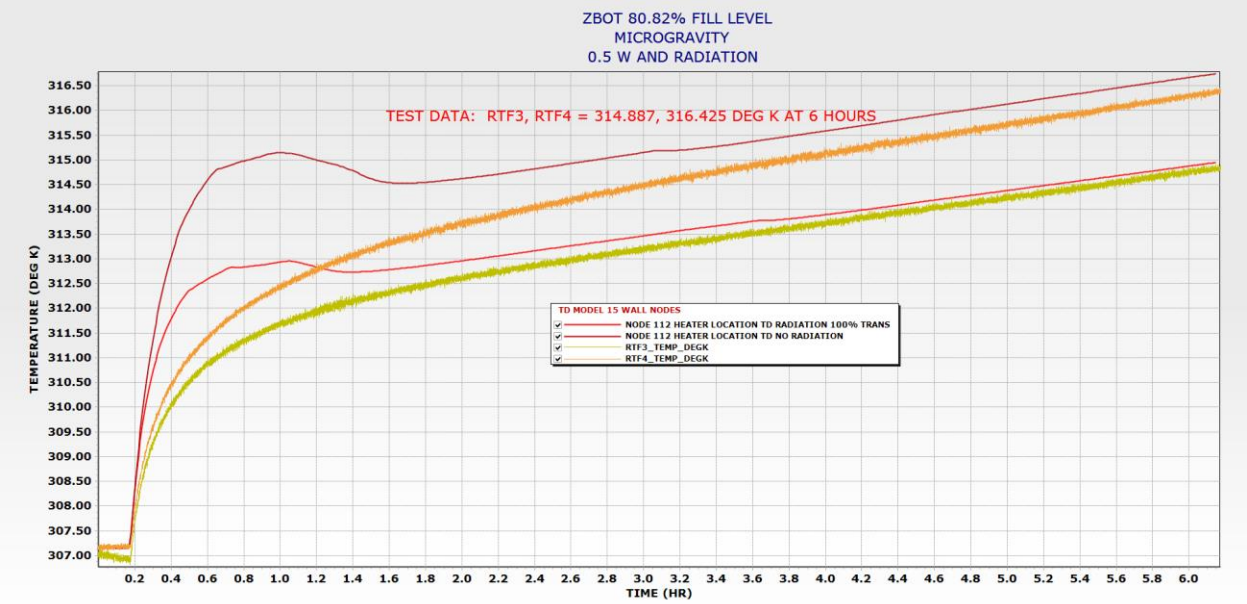

Figure A20: ZBOT Self-Pressurization Case Wall Temperature at Heater Location Versus Time for 0% and 100% Rates of Radiation Transmission through Perfluoropentane for TD Model

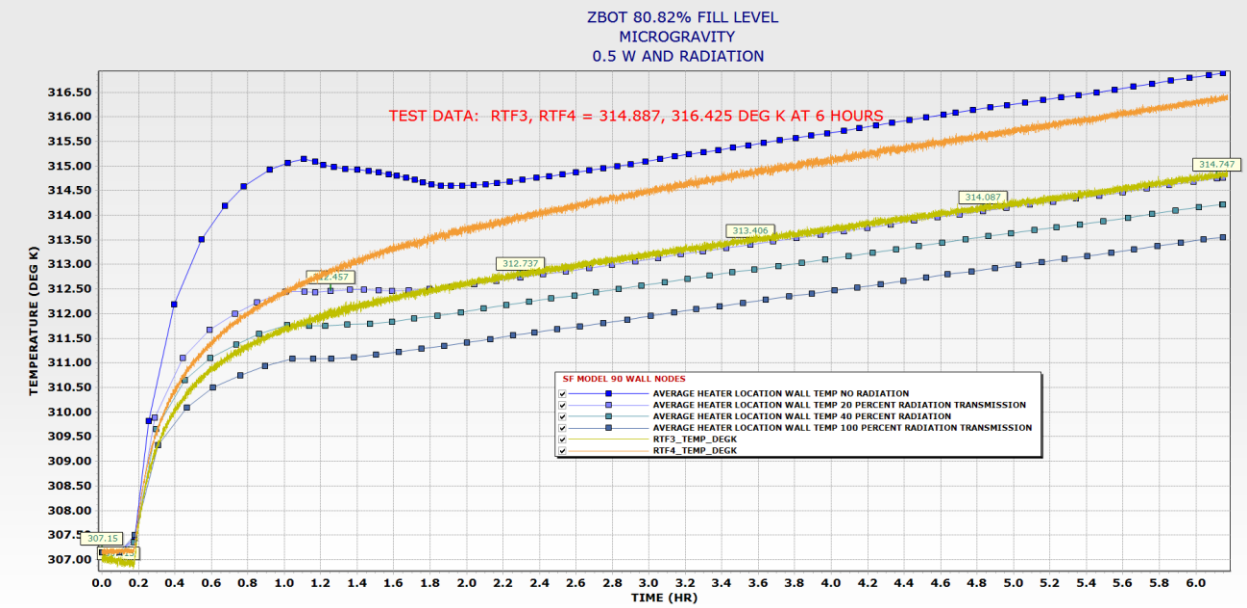

Figure A21: ZBOT Self-Pressurization Case Wall Temperature at Heater Location Versus Time for Various Rates of Radiation Transmission through Perfluoropentane for SF Model

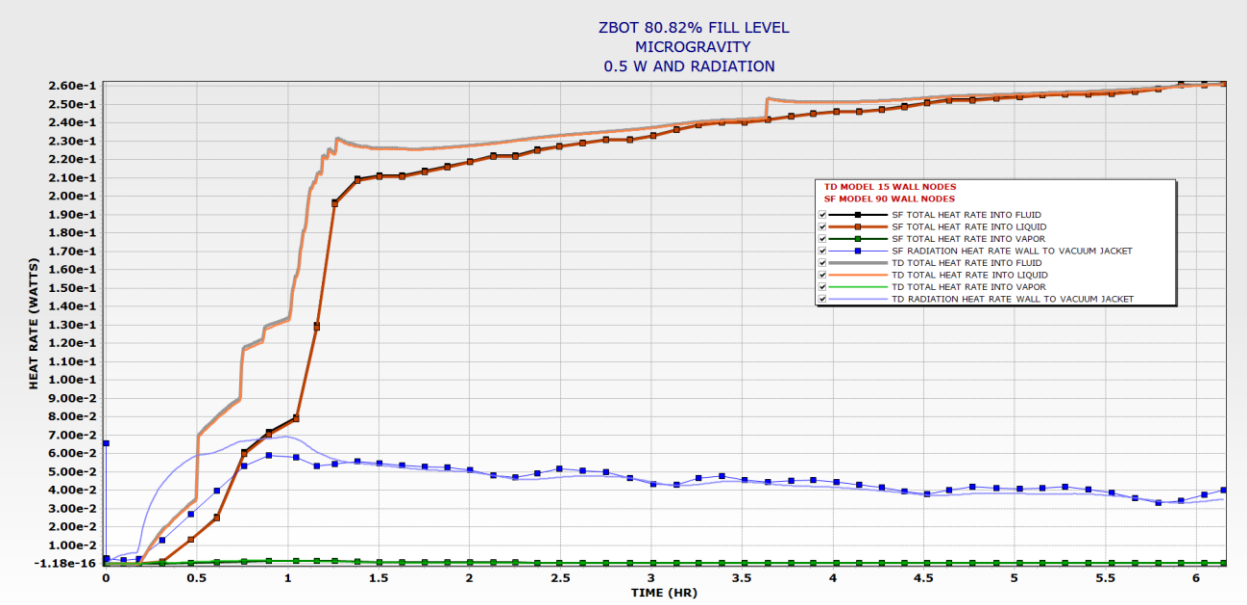

Figure 22: ZBOT Self-Pressurization Case Heat Rate Comparison between TD and SF Models

ZBOT Self-Pressurization Case 1 g 1.0 Watts Strip Heater

The fill level for this ZBOT 1g self-pressurization case was 90%. Figure 23 shows the pressure results from the SF model compared to test data for 20% and 40% rates of transmission through perfluoropentane in the tank. Results compare reasonably well to test data.

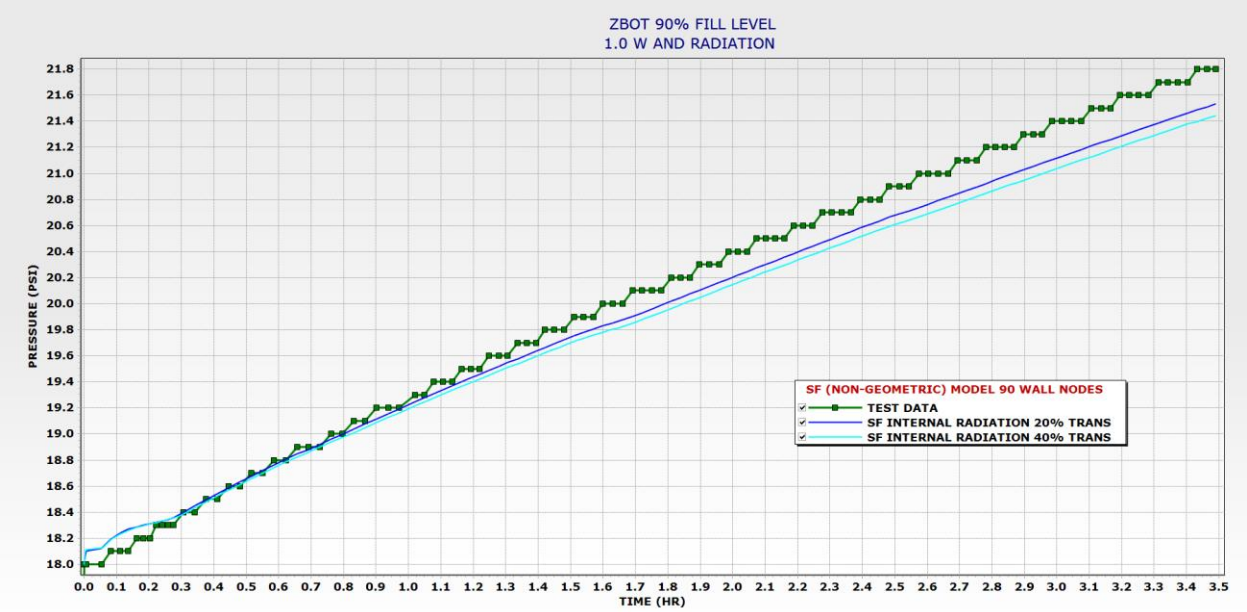

Figure 23: ZBOT Self-Pressurization Case Pressure Versus Time for 20% and 40% Rates of Radiation Transmission through Perfluoropentane for SF Model

IV. Conclusion

It was demonstrated that a one-dimensional multi-nodal approach to modelling self-pressurization in microgravity and 1g is very effective. This one-dimensional multi-nodal model also is effective in modelling jet mixing in microgravity and 1g. Run times for the SF models averages at about a couple of hours for the self-pressurization and jet mixing. The models using the TD interface take approximately 12 hours. The SF and TD models compare favorably to each other in terms of calculating radiation heat rates internally in the tank and externally to a given environment. Temperature and Pressure results between the two models are also comparable. It was found that in microgravity there was a delay time before free convective heat transfer dominates over pure conduction heat transfer within the tank. It was found that perfluoropentane was not completely opaque in the IR range, thereby allowing some radiation transmission within the tank, which not surprisingly affected the microgravity cases more than the 1g cases. Finally a working interface to link the tank stratification model in SINDA/FLUINT to Thermal Desktop was developed so that more complex tanks and their environments could be modelled.

V. Nomenclature

c_p = specific heat at constant pressure, J/(kg·K)
C = geometric scaling factor
djet = jet submergence, m
D = diameter of tank, m
F = multiplication factor on geometric scaling factor
g = gravity, m/s^2
h = enthalpy, J/kg
h_{fg} = latent heat, J/kg
H = height or characteristic length, m
Ja = Jacob number $1/(h_{fg}/ c_p(T_{int}-T_{jt}))$
k = thermal conductivity, W/(m·K)
m = mass flow rate, kg/s

Nu = Nusselt number, hD/k
Pr = Prandtl number, $C_p\mu/k$
Q = heat rate, W
Ra = Rayleigh number
Re = Reynolds number, GD/μ
St = Stanton number
tcv = time to convect, s
T = temperature, K
ΔT = temperature difference, K
U = Velocity, m/s
V = Turbulent Velocity at Interface, m/s
α = thermal diffusivity, m^2/s
β = coefficient of thermal expansion, K
δ = boundary layer thickness
μ = dynamic viscosity, Pa·s
ρ = density, kg/m^3
ν = kinematic viscosity, m^2/s
σ = surface tension, N/m

Subscripts

b = buoyancy
int = liquid/vapor interface
j = jet
LU = SF LUMP
str = strip heater
w = wall

VI. References

1. Sakowski, B. "SINDA/FLUINT Stratified Tank Modelling" *TFAWS 2014 Proceedings* NASA Glenn Research Center, Cleveland, OH.

2. Kassemi, M., Hylton, S., Kartuzova, O. "Zero-Boil-Off-Tank (ZBOT) Experiment – Ground-Based Validation of Two-Phase Self-Pressurization CFD Model & Microgravity Results" *2018 Joint Propulsion Conference, AIAA Propulsion and Energy Forum, (AIAA 2018-4940),* Cincinnati, Ohio.

3. Bejan, Adrian, "Convective Heat Transfer", John Wiley & Sons Inc., 2004 pp 247.

4. Simons, J.H., "Flourine Chemistry: Volume 2", Elsevier, December 2012.

5. Bravo, I., Aranda, A., Hurley, M.D., Marston, G., Nutt, D.R., Shine, K.P., Smith, K., Wallington, T.J., "Infrared Absorption Spectra, Radiative Efficiencies, and Global Warming Potentials of Perfluorocarbons: Comparison Between Experiment and Theory" JGR Atmospheres, Volume 115, Issue D24, 27 December 2010.

6. Lin, C.S., Hasan, M.M., Nyland, T.W., "Mixing and Transient Interface Condensation of a Liquid Hydrogen Tank", 29th *Joint Propulsion Conference and Exhibit, (AIAA 1993-1968),* Monterey, California, June 28-30, 1993.